

# Effect of grain boundary structure on the intercrystalline damaging of austenitic steel during brazing

Kornél Májlinger / Péter János Szabó

Received 2011-11-31

## Abstract

During brazing of austenitic stainless steel with copper based brazing material a common failure occurs, namely that the brazing material solutes along grain boundaries, which looks like cracks. This unfortunate effect occurred when AISI 304 and 310 steels are brazing. To avoid this unwanted effect – since the cracks propagate mainly on high angle grain boundaries – our goal was to enhance the number of special coincident site lattice type grain boundaries with thermomechanical treatment. Experiments were performed for 1, 48 and 72 hour heat treatments on materials cold rolled at different levels. After the thermomechanical treatment significant decrease in the crack size was found in depth and width, respectively.

## Keywords

austenitic steel · copper brazing · intercrystalline cracking · electron backscatter diffraction

## Acknowledgement

This work is connected to the scientific program of the “Development of quality-oriented and harmonized R+D+I strategy and functional model at BME” project, and this project is also supported by the New Hungary Development Plan (Project ID: TÁMOP-4.2.1/B-09/1/KMR-2010-0002). P. J. Szabó is grateful for the support of Bolyai János Scholarship. The results discussed above are also supported by the grant TÁMOP-4.2.2.B-10/1–2010-0009.

Kornél Májlinger

Péter János Szabó

Department of Materials Science and Engineering, BME, H-1111 Budapest, Bertalan Lajos utca 7, Hungary

## 1 Introduction

Corrosion resistant and stainless steels are widely used in the industry. Austenitic stainless steels, one group of such steels are often applied in the automotive industry [1]. Many cases it is necessary to join austenitic parts air-proofly, for which welding and brazing are good solutions. Brazing is a fast and efficient way for joining such parts for low mechanical loads, for example in the case of exhaust systems of cars. For such applications, AISI 304 stainless steel is widely used due to the combination of good mechanical properties and excellent corrosion resistance over a large temperature range. To braze austenitic stainless steels mostly copper based braze materials are used. If AISI 304 steel is brazed with Boehler SG-CuSi3 brazing material, long intercrystalline cracks occur in the steel, full with copper (Fig. 1). This effect is similar to the intergranular corrosion of austenitic steels. Intergranular corrosion can be prevented or improved by increasing the fraction of so-called special grain boundaries [2–4].

Grain boundaries can be classified from different point of views. One popular division is based on the properties of the grain boundaries. The random or general boundaries are characterized by average values for specific parameters (energy, etc.). On the other hand there are so called special boundaries having values for specific parameter(s) which are very different from the values of the random boundaries. These differences are caused by the special geometry of the boundary.

The grain boundaries which have a given fraction of atoms in the grain boundary plane which are coincident to both lattices separated by the grain boundary are characterized by the Coincident Site Lattice (CSL) model [5]. These boundaries are classified in terms of  $\Sigma$  values. The  $\Sigma$  value denotes the fraction of atoms in coincidence, e.g. in a  $\Sigma 3$  boundary every third atom is at coincident site. There are often multiple misorientations that can achieve a given  $\Sigma$  value. For example  $\Sigma 33$  can be achieved by a 20.05 degree rotation about [110], or 33.56 degrees about [311], or 58.99 about [110]. These three descriptions may be combined in the distribution. The frequency of  $\Sigma 3$  and  $\Sigma 3^n$  type CSL-boundaries is much higher than that of other CSL-boundaries and they play an important role in the tun-

ing of material properties [5]. By increasing the number of the CSL-boundaries better corrosion and fatigue properties can be obtained [2], [5–7]. To increase the fraction of CSL boundaries several thermomechanical treatments are known [2–5], [8–10].

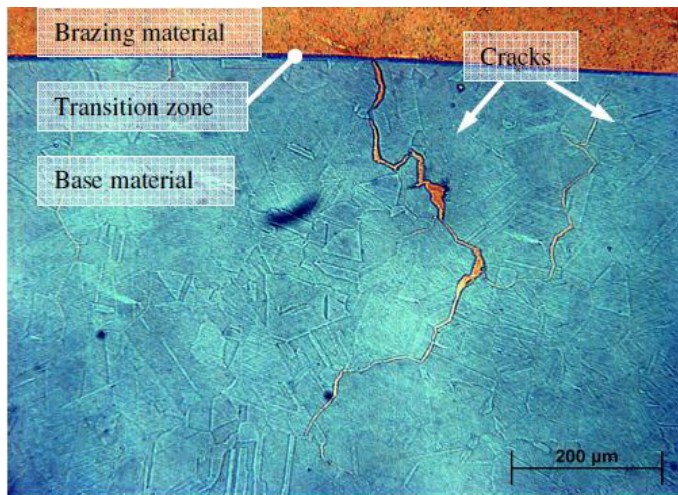


**Fig. 1.** Light microscope image of the cross section of a MIG brazed specimen (304\_as\_rec).

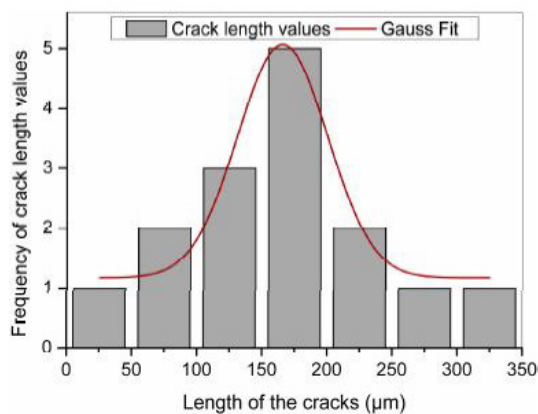


**Fig. 2.** Histogram of the crack length values of sample 304\_5\_1h in width direction and the fitted Gauss curve

## 2 Experimental

The brazing experiments with 1mm BoehlerSG-CuSi3 (2.1461) MIG brazing wire (for chemical composition see Tab. 1) were made on the surface of AISI 304 and AISI 310 austenitic steel pieces (for chemical composition see Tab. 2 Tab. 3) with initial cross section of  $10 \times 10 \text{ mm}^2$ .

The parameters for the MIG brazing were: alternating-current; 56 A, voltage 17 V, the wire feed was 4.4 m/min. As shielding gas 30 % He – 70 % Ar mixture with 10 l/min flow was applied.

First the as received material was investigated. To increase the ratio of special CSL grain boundaries thermomechanical treatments were made. The austenitic samples were cold rolled with different plastic deformation rate  $\phi$ , and then annealed at  $950^\circ\text{C}$  in a furnace for different times. The plastic deformation rates and annealing times are listed in Tab. 4.

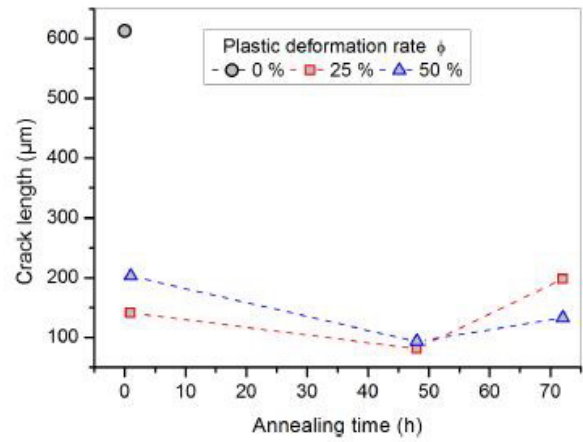


**Fig. 3.** Crack length into the surface (depth) according the plastic deformation rate and the annealing time for AISI 304 steel

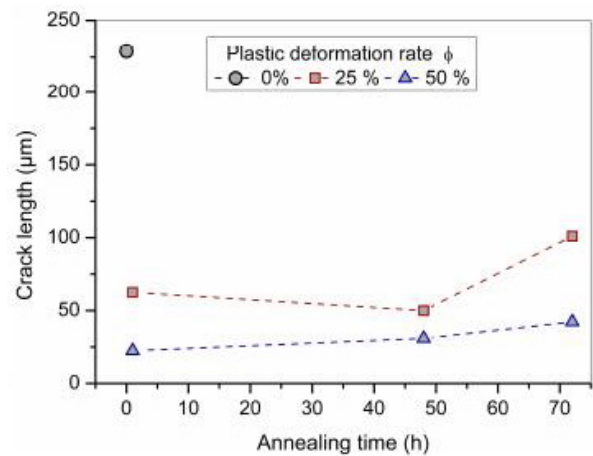


**Fig. 4.** Crack length into the surface (depth) according the plastic deformation rate and the annealing time for AISI 310 steel

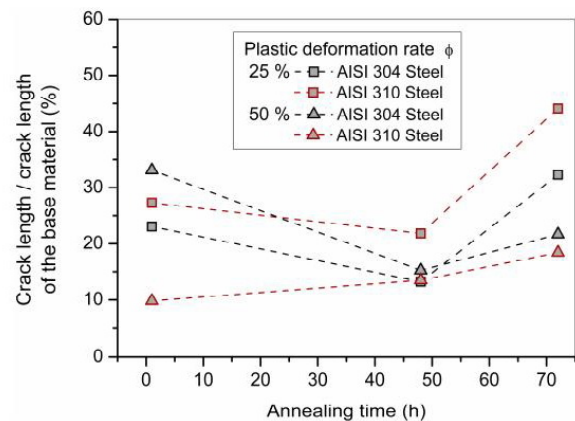


**Fig. 5.** Crack length/crack length of the base material ratio (in depth) according the plastic deformation rate and the annealing time for AISI 304 and AISI 310 steels

## 3 Measurements

To quantify the effect of thermomechanical treatment on the crack propagation, the typical sizes of the cracks were determined as described below. Light microscope images were taken from the whole cross section of the brazed and metallographically prepared samples. The depth (normal to the brazed sur-

**Tab. 1.** Chemical composition of the SG-CuSi3 Brase wire (wt%)

Si	Mn	Fe	Sn	Cu
2.9	1	≤0.3	≤0.2	bal.

**Tab. 2.** Chemical composition of the AISI 304 Steel (wt%)

C	Si	Mn	P	S	Cr	Mo	Ni	V	Al	Cu	W	Ti	Co	Pb	Fe
≤0.08	≤1	≤2	≤0.045	≤0.03	18-20	≤0.15	8-11	≤0.1	≤0.1	≤0.3	≤0.1	≤0.05	≤0.1	≤0.15	bal.

face) and width (parallel to the brazed surface) of every crack on the samples were measured with image analysis software. Then the frequency of crack length values was calculated and displayed in a histogram with a dedicated software. After this, different curves were fitted to the diagram. The Gauss curve was found to fit the best for the values (see for example Fig. 2) so the crack length was determined by this function.

To see the grain boundary characteristics electron backscattered diffraction (EBSD) measurements were made on the AISI 304 samples with a Philips XL 30 scanning electron microscope equipped with a TSL TexSEM EBSD-detector system. The scanned area at the border of the brazed region was approx.  $300 \times 290 \mu\text{m}^2$  with  $1,7 \mu\text{m}$  step size. The EBSD measurements were made on the cross section of the samples prepared by traditional method [11].

#### 4 Results and discussion

Crack sizes determined after brazing of the as received material and the thermomechanical treated samples are listed in Tab. 5.

In case of the ASI 304 steel it can be clearly seen that the average crack length decreased significantly after the thermomechanical treatments. In every case the crack depth reduced at least one third of that of the untreated sample (Fig. 3). The best result was achieved after 48 h of heat treatments, when the initial crack depth of the untreated sample ( $613 \mu\text{m}$ ) was reduced by one sixth ( $100 \mu\text{m}$ ). After 72 h treatments the crack depths increased slightly, but were significantly smaller than that of the untreated sample. The crack width values also decreased after the thermomechanical treatments, but with less rate than the crack depth values.

In case of the ASI 310 steel it it can be clearly seen that the average crack length decreased significantly after the thermomechanical treatments. In every case the crack depth reduced to half of that of the untreated sample (Fig. 4). The best result was achieved after 1 h heat treatment with 50 % plastic deformation, when the initial crack depth of the untreated sample ( $229 \mu\text{m}$ ) was reduced by one tenth ( $23 \mu\text{m}$ ). After 72 h treatments the crack depths increased slightly, but were significantly smaller than that of the untreated sample. The crack width values also decreased after the thermomechanical treatments, but with smaller rate than the crack depth values.

It is clear that the 301 material is much less affected by the

intercrystalline cracking, it has significantly smaller cracks in both directions and thus it is more corrosion resistant also.

To see the effect of the heat treatment for decreasing the crack length in Fig. 5. the *crack length / crack length of the base material* ratio is shown for both steels and thermomechanical treatments. All the treatments decreased the crack length in the austenitic samples. The best result was achieved by the 1 h 50 % plastic deformation rate for the 310 steel. in the other cases generally the 48 h treatment decreased most the crack length ratio, and in the case of 72 h treatments a increase in the crack length occurred. For all the samples the crack length ratio was under 50 %. The SEM-EBSD measurements for the AISI 304 steel showed, that the intercrystalline cracks propagate mostly along the random grain boundaries (e.g. Fig. 6). In Tab. 6 the length fraction of the different grain boundary types measured by EBSD can be seen. It is clear, that the fraction of the CSL grain boundaries increased significantly after every thermomechanical treatment. Thus the CSL/(random high angle grain boundary) fraction increased too. The fraction of twin ( $\Sigma 3$  CSL) grain boundaries also increased after thermomechanical treatment.

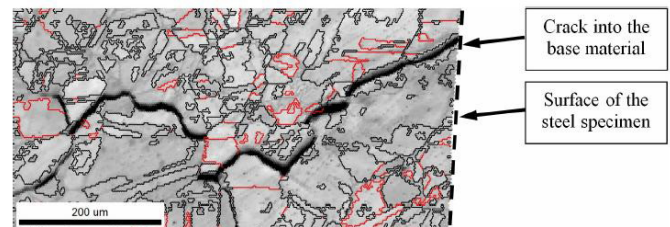


**Fig. 6.** Image quality map with grain boundaries. Random high angle boundaries (black), CSL boundaries (red) (304\_as\_rec)

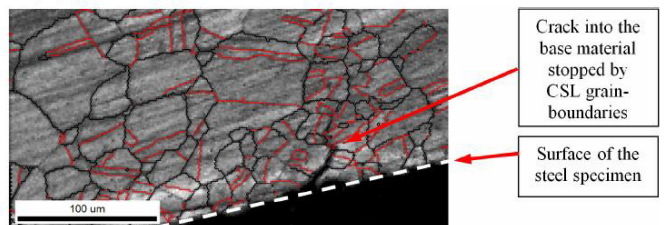


**Fig. 7.** Image quality (IQ) map of a thermomechanically treated sample with grain boundaries (304\_50\_72h). Random high angle boundaries are black, CSL boundaries are red

This increase of the fraction of special gain boundaries decreased the average crack depth after braze process significantly.

**Tab. 3.** Chemical composition of the AISI 310 Steel (wt%)

C	Si	Mn	P	S	Cr	Mo	Ni	V	Al	Cu	W	Ti	Co	Pb	Fe
≤0.25	≤1.5	≤2	≤0.045	≤0.03	24-26	≤0.15	19-22	≤0.1	≤0.1	≤0.3	≤0.1	≤0.05	≤0.1	≤0.15	bal.

**Tab. 4.** Parameters of the thermomechanical treatment

Sample(AISI 304)	Sample(AISI 310)	plastic deformation rate $\phi$ (%)	annealing time(h)
304_as_rec.	310_as_rec.	-	-
304_25_1h	310_25_1h	25	1
304_25_48h	310_25_48h	25	48
304_25_72h	310_25_72h	25	72
304_50_1h	310_50_1h	50	1
304_50_48h	310_50_48h	50	48
304_50_72h	310_50_72h	50	72

**Tab. 5.** Crack sizes after brazing for AISI 304 and AISI 310 steels

Sample	Crack sizes( $\mu\text{m}$ )		Sample	Crack sizes( $\mu\text{m}$ )	
	Depth	Width		Depth	Width
304_as_rec	613	247	310_as_rec	229	61
304_25_1h	141	76	310_25_1h	63	31
304_25_48h	81	54	310_25_48h	50	8
304_25_72h	198	175	310_25_72h	101	40
304_50_1h	203	166	310_50_1h	23	6
304_50_48h	93	64	310_50_48h	31	23
304_50_72h	133	51	310_50_72h	42	9

**Tab. 6.** Length fraction of the different grain boundary types measured by EBSD

Sample	Length fraction of grain boundaries				
	Random high angle	CSL	Twin	CSL/twin	CSL/random high angle
304_as_rec.	0,808	0,123	0,024	5,125	0,152228
304_25_1h	0,957	0,470	0,157	2,993631	0,491118
304_25_48h	0,999	0,456	0,138	3,304348	0,456456
304_25_72h	0,970	0,498	0,223	2,233184	0,513402
304_50_1h	0,913	0,440	0,290	1,517241	0,481928
304_50_48h	0,926	0,471	0,263	1,790875	0,508639
304_50_72h	0,879	0,463	0,357	1,296919	0,526735

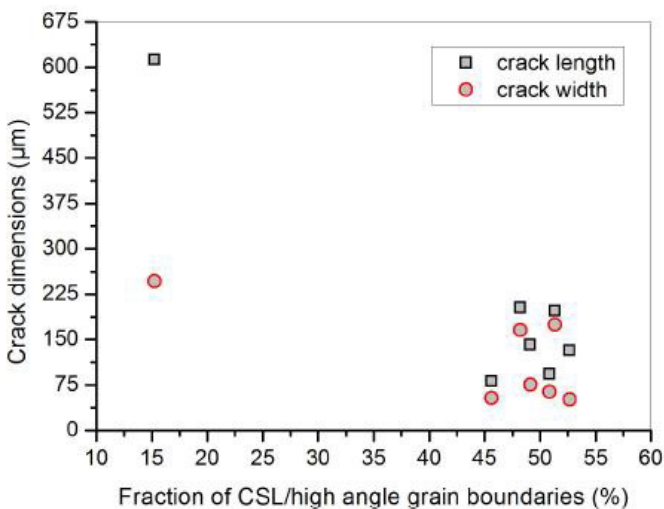


**Fig. 8.** Crack length and width into the surface versus the fraction of CSL/random high angle grain boundary (AIS 304 samples)

In Fig. 7. it can be clearly observed as a CSL boundary stops the propagation of a crack.

In Fig. 7 the dimensions of cracks are plotted *versus* the frac-

tion of CSL/random high angle grain boundaries. A clear decrease in crack size with the increased CSL/random high angle fraction can be observed.

### 5 Conclusion

Due to their higher *Cr* and *Ni* content the more corrosion resistant AISI 310 steel is much less effected by the intercrystalline cracking than the AISI 304 steel.

In the case of the AISI 304 steel the relative fraction of CSL grain boundaries to the total amount of grain boundaries increased due to the thermomechanical treatments. The relative fraction of CSL grain boundaries to the amount of random high angle grain boundaries increased significantly due to the thermomechanical treatments. The average crack dimensions decreased significantly after brazing the thermomechanical treated samples, because the CSL grain boundaries, due to their lower surface energies, stopped and blocked the intercrystalline crack propagation.

## References

- 1 **Davis JR**, *Stainless Steels New York: An ASM Specialty Handbook*, ASM International, 1994.
- 2 **Hu C, Xia S, Li H, Liu T, Zhou B, Chen W, Wang N**, *Improving the intergranular corrosion resistance of 304 stainless steel by grain boundary network control*, *Corr. Sci* **53** (2011), no. 5, 1880–1886, DOI 10.1016/j.corsci.2011.02.005.
- 3 **Zhou Y, Aust KT, Erb U, Palumbo G**, *Effects of grain boundary structure on carbide precipitation in 304L stainless steel*, *Scripta Mater* **45** (2001), no. 1, 49–54, DOI 10.1016/S1359-6462(01)00990-3.
- 4 **Kumar M, Schwartz AJ, King WE**, *Microstructural evolution during grain boundary engineering of low to medium stacking fault energy fcc materials*, *Acta Mater* **50** (2002), no. 10, 2599–2612, DOI 10.1016/S1359-6454(02)00090-3.
- 5 **Tan L, Sridharan K, Allen TR, Nanstad RK, McClintock DA**, *Microstructure tailoring for property improvements by grain boundary engineering*, *J. Nucl. Mater* **374** (2008), no. (1–2), 270–280, DOI 10.1016/j.jnucmat.2007.08.015.
- 6 **Shimada M, Kokawa H, Wang ZJ, Sato YS, Karibe I**, *Optimization of grain boundary character distribution for intergranular corrosion resistant 304 stainless steel by twin-induced grain boundary engineering*, *Acta Mater* **50** (2002), no. 9, 2331–2341, DOI 10.1016/S1359-6454(02)00064-2.
- 7 **Tsurekawa S, Nakamichi S, Watanabe T**, *Correlation of grain boundary connectivity with grain boundary character distribution in austenitic stainless steel*, *Acta Mater* **54** (2006), no. 13, 3617–3626, DOI 10.1016/j.actamat.2006.03.048.
- 8 **Kurban M, Erb U, Aust KT**, *A grain boundary characterization study of boron segregation and carbide precipitation in alloy 304 austenitic stainless steel*, *Scripta Mater* **54** (2006), no. 6, 1053–1058, DOI 10.1016/j.scriptamat.2005.11.055.
- 9 **Myrjam W**, *Grain boundary engineering by application of mechanical stresses*, *Scripta Mater* **54** (2006), no. 6, 987–992.
- 10 **Schwartz AJ, King WE, Kumar M**, *Influence of processing method on the network of grain boundaries*, *Scripta Mater* **54** (2006), no. 6, 963–968, DOI <http://dx.doi.org/10.1016/j.scriptamat.2005.11.052>.
- 11 **Vander VG, Dillon S, Manilova E**, *Metallographic Preparation for Electron Backscattered Diffraction*, *Micros. Microanal* **12** (2006), 1610–1611.